Possible Design Modification for Capacitive Type MEMS Accelerometer

Dr. Jyoti K. Sinha
School of Mechanical, Aerospace and Civil Engineering
Manchester University

Dr. Ramadan E. Gennish
Department of Mechanical Engineering- Faculty of Engineering
Zawia University

Dr. Abdellatef E. Albadri
Department of Maintenance Engineering – Libyan air lines
Tripoli Airport

Abstract:

The use of Micro-Electro Mechanical System (MEMS) concept for manufacturing accelerometers is relatively new technology. However earlier studies suggest that the measured signals by the MEMS accelerometers generally show deviation when compared with the conventional accelerometer. Hence, a simple Finite Element (FE) model of a MEMS accelerometer has been constructed and the modal analysis has been carried out. The cantilever beam mode of finger used in MEMS capacitive type accelerometers observed in the modal analysis highlights the possibility of errors in measurement which is clearly due to non-parallel plates affect. Hence, few modifications in finger design have been

suggested to improve the performance of the MEMS accelerometer. The proposed finger shape provided the rigid body motion which is required to give parallel plates during the finger movements and eliminates the non-parallel effect.

Keywords: MEMS Accelerometer; Vibration Measurement; Finite Element (FE) Analysis; Modal Analysis; MEMS Accelerometer Design.

1. Introduction:

The MEMS (Micro-Electro Mechanical System) accelerometers have been receiving attention in the recent years due to their low cost and small size [1-2]. The micromachined accelerometer was initially introduced in 1988 by Nova Sensor which was based on piezoresistive sensing mechanism [1]. It was based on the Wheatstone bridge principle to measure the acceleration of vibrating objects [1, 3-4]. Thereafter the concept of capacitive sensing has also been introduced in the MEMS accelerometers [5-10]. A typical capacitive MEMS accelerometer is composed of capacitors formed between the proof mass and fixed conductive electrodes. The proof mass is free to move in the vibration direction. This mass movement creates unbalance in the differential capacitor resulting in an output which is proportional to acceleration of the vibrating object. The capacitance change due to acceleration is then converted into voltage with appropriate signal conditioning through on chip circuitry [5-10]. Sections 2 and 3 briefly discussed the principle of a conventional piezoelectric accelerometer and the capacitive type MEMS accelerometer.

However, the performance of such accelerometers has not been rigorously tested to enhance the confidence level for the industrial

applications. A few earlier researches gave comparison of the performance between the MEMS and conventional accelerometers. It has been observed that the measured vibration signals by the MEMS accelerometer often show difference when compared with the signals measured by the well-accepted conventional accelerometer [11-13]. Hence the present attempt is to understand the dynamics of the present design used for the MEMS accelerometer so that appropriate modification either in the mechanical design or in the associated electronic circuitry can be proposed to improve the performance of the MEMS accelerometer in future. In the present study the dynamic behaviour of the sensing element of capacitive type MEMS accelerometer has been studied. Hence, a simple Finite Element (FE) model of a MEMS accelerometer has been constructed and the modal analysis has been carried out. The cantilever beam mode of finger used in MEMS capacitive type accelerometers observed in the modal analysis highlights the possibility of errors in measurement. Hence, few modifications in finger design have been suggested to improve the performance of the MEMS accelerometer.

2. Conventional Piezoelectric Accelerometer:

A typical design of a conventional piezoelectric accelerometer is shown in Figure 1. It consists of a small mass, a spring made of piezoelectric crystal and a damping of around 0.7. For this configuration, if the natural frequency of the accelerometer is f_n then the linearly frequency range of measurement is approximately 20% of the natural frequency, f_n.

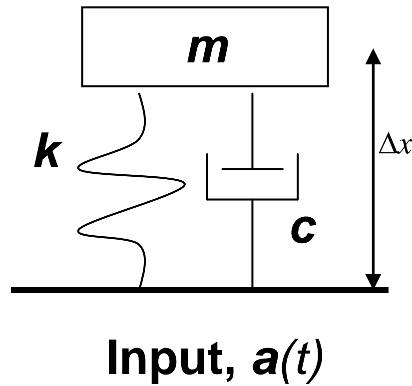

Figure 1 Conventional piezo-electric accelerometer

The input acceleration of a vibrating object causes the vibration of the accelerometer mass, m which results in the relative motion, $\Delta x(t)$, between the mass and the object in the piezoelectric spring generates the proportional electric charge, $\Delta Q(t)$. Mathematically it can be written as

$$\Delta x(t) \approx \frac{a(t)}{\omega_n^2} \propto \Delta Q(t) \tag{1}$$

where $\omega_n = 2\pi f_n$. Hence the charge, $\Delta Q(t)$, is proportional to the acceleration of the vibrating object which is then converted into the voltage as the output for the accelerometer.

3. Capacitive type MEMS Accelerometer:

The working principle of a capacitive type MEMS accelerometer is the same as the conventional piezoelectric accelerometer. However the output of the MEMS accelerometer uses the change in the capacitance and not to the charge. A typical design configuration of a MEMS accelerometer is shown in Figure 2 [14].

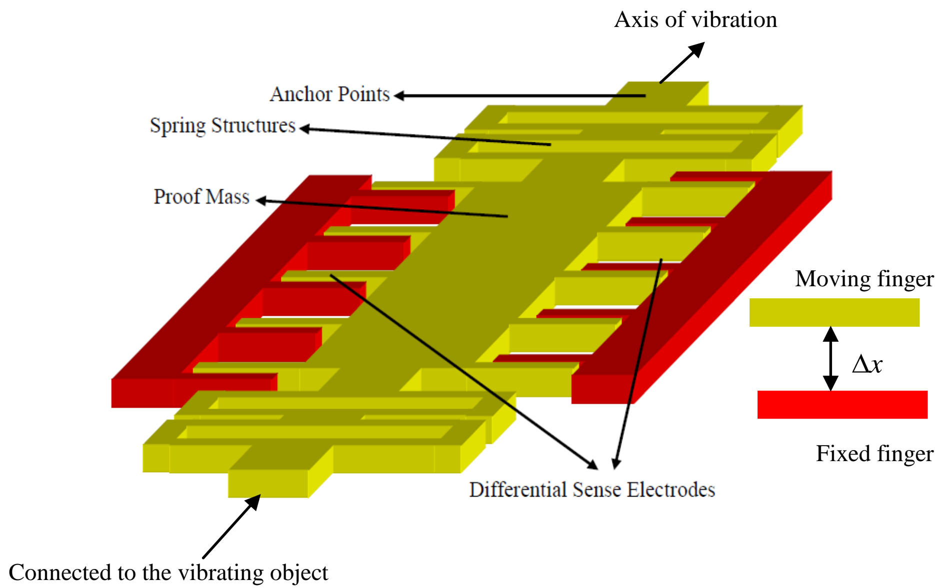

Figure 2 Typical constructional details of a capacitive type MEMS accelerometer [14]

The MEMS accelerometer also consists of a spring and a mass both made of a material commonly poly-silicon. However, the concept of converting the mechanical vibration to electrical signal is different. Here numbers of fingers are attached to the mass which is generally called as the "Moving fingers" and number of fingers attached to the fixed frame of the accelerometer, called "Fixed fingers". The arrangement is such that a pair the fixed and moving fingers constitutes a parallel capacitor. Here again, the input acceleration of a vibrating object causes the vibration of the accelerometer mass, m which results in the relative motion, $\Delta x(t)$, between the moving and fixed fingers which generates the proportional change in the capacitance, $\Delta C(t)$. Mathematically it can be written as,

$$\Delta x(t) \approx \frac{a(t)}{\omega_n^2} \propto \Delta C(t) \qquad (2)$$

where the change in the capacitance, $\Delta C(t) = C_0 \cdot (\frac{\Delta x(t)}{d_0})$ [10] . The capacitance $\Delta C(t)$ is proportional to the acceleration of the vibrating object which is then converted into the voltage as the output for the accelerometer. Often number of the fixed and moving fingers is used to strengthen the electrical and therefore the sensitivity of the accelerometer.

4. MEMS Accelerometers Performance:

Performance tests for several MEMS accelerometers have been carried out using test set-up shown in Figure 3 [13, 15, and 16]. The test setup consists of a small shaker (M/s GW make) together with a shaker power amplifier, signal generator and a PC based data acquisition for data collection and storage for further signal processing. In every test the MEMS accelerometer (Test accelerometer) was attached back to back with an Integrated Circuit Piezoelectric (ICP) conventional accelerometer (Reference accelerometer) on the armature of the shaker.

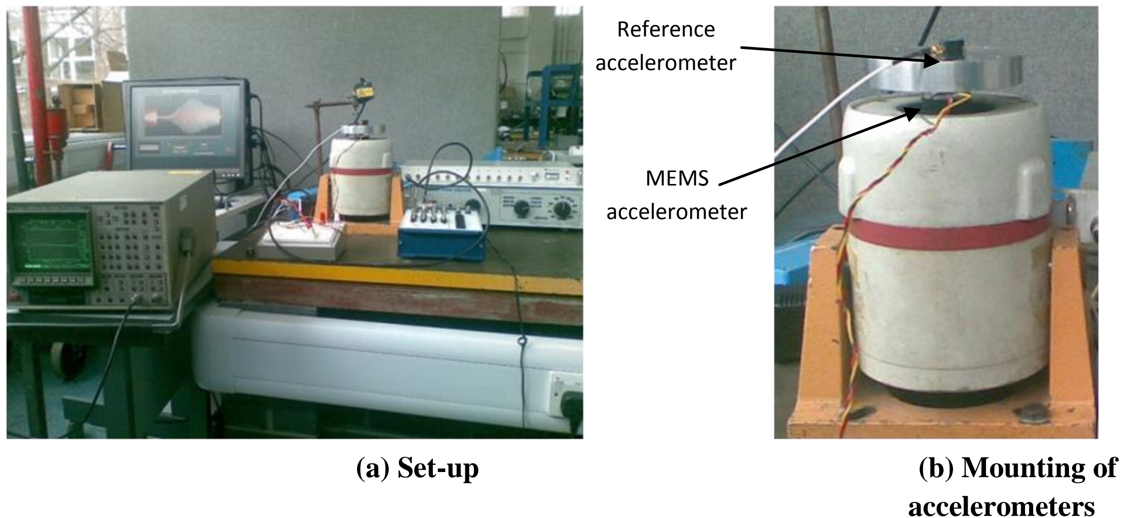

(a) Set-up **(b) Mounting of accelerometers**

Figure 3 Test facilities

Responses of MEMS accelerometers showed significant deviation in both amplitude and phase compared to the responses of the reference accelerometer and this deviation is changing with the frequency. A few typical examples for measured responses of MEMS accelerometers compared with the reference accelerometer are shown in Figures 4 to 6 for the impulsive, random and sinusoidal excitations respectively.

A typical example on a rotating rig in Figure 7 also shows deviation in the MEMS measurement compared to the measurement by the conventional accelerometer which is shown in Figure 8.

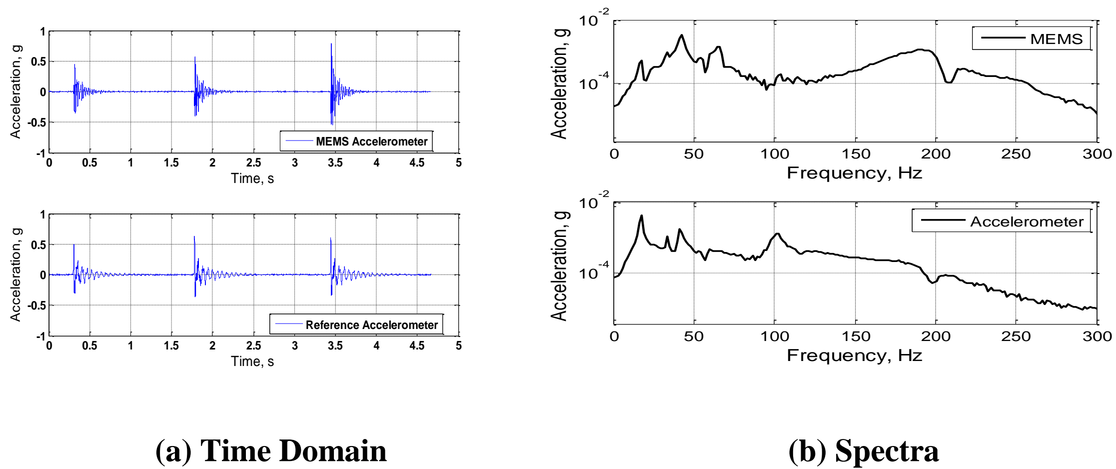

(a) Time Domain **(b) Spectra**

Figure 4 Measured responses for impulsive excitation

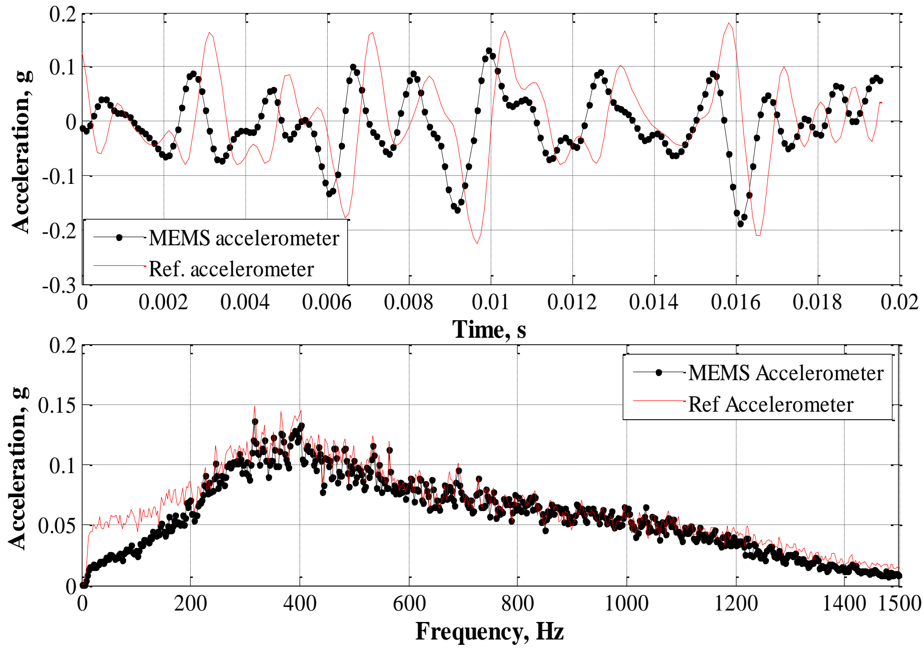

Figure 5 Measured responses for the random excitation

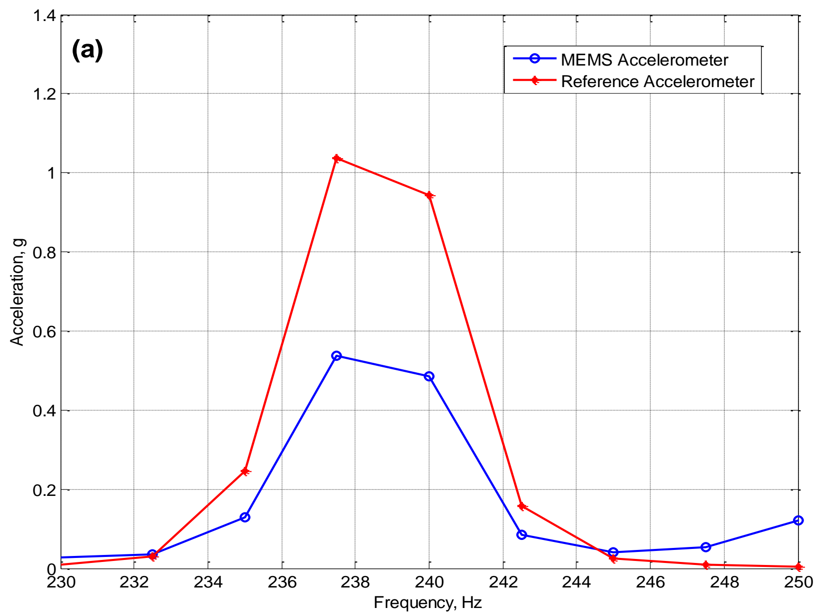

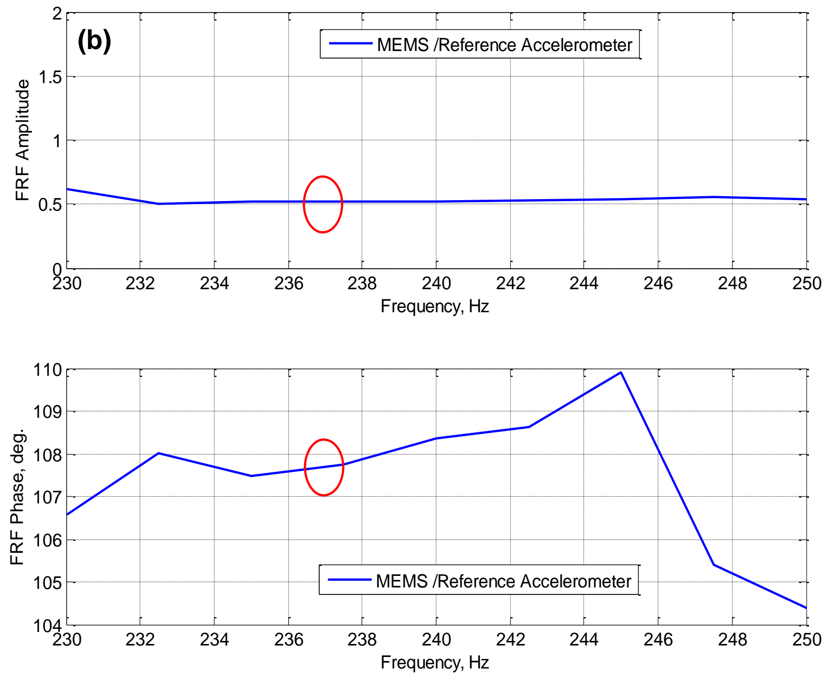

Figure 6 (a) measured responses for the sinusoidal excitation at 237 Hz, (b) Amplitude and phase of FRF

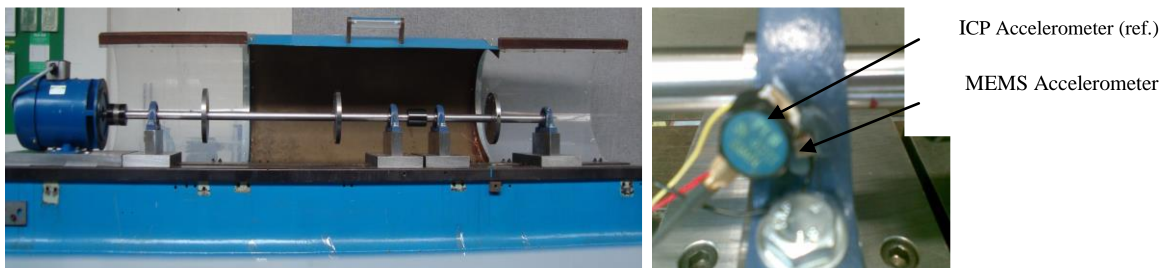

Figure 7 motor test rig

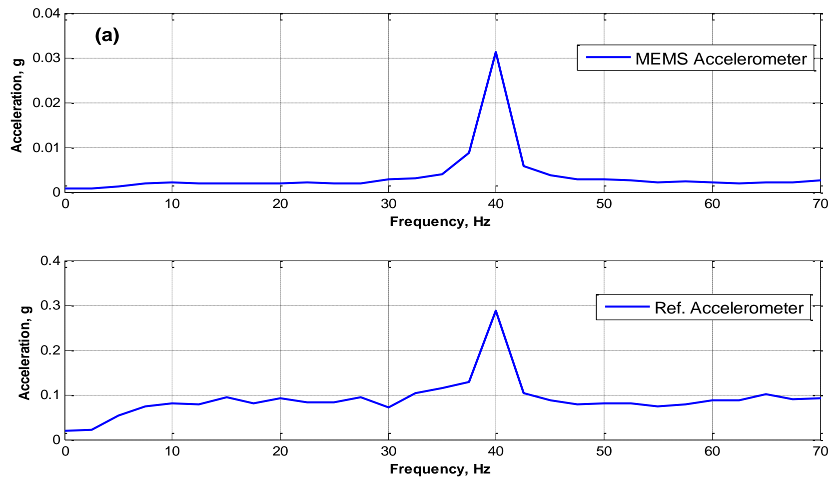

Figure 8 (a) spectra for measured responses of MEMS and reference accelerometers at 2400rpm

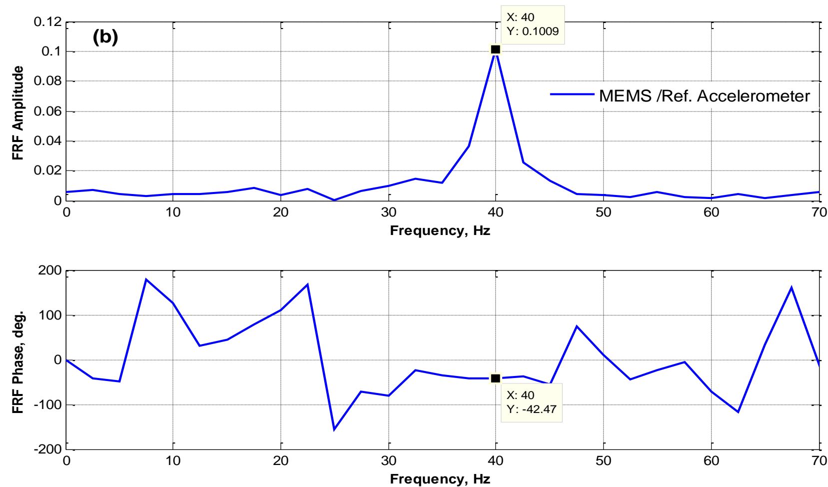

Figure 8 (b) amplitude and phase of FRF at 2400 rpm

It has been observed that the frequency contents in the spectra of the MEMS accelerometers are the same as the conventional reference accelerometer; however the amplitude and phase at each frequency

significantly different, when compared with the conventional reference Accelerometer. Due to the similarity in principle or operation and difference in change in the output as explained previously in sections 2 and 3. A couple of methods have been suggested earlier [15, 16] to improve the measured signals of the MEMS accelerometers. However it is always good to understand the dynamics of the MEMS accelerometer to know the reason for such error so that the possible improvement in the design can be made.

4. 3D Finite Element model :

The typical design configuration shown in Figure 2 has been modelled in 3D, but only two moving fingers of 154 µm length and 4 µm width have been used. Three fixed fingers of the same moving fingers dimensions are attached to the mass which is 28µm of length and 152 µm width. The gap between each moving finger and fixed finger is 4µm.The mass is fixed to the frame through two folded beams one on the top and other on the bottom. The element type used in this model is Continue 3-Dimensions 4 node (C3D4), material properties of polysilicon used are, density $\rho = 2.3 g/cm^3$, Poisson's ratio=0.22, and Young's modulus $E = 170 GPa$. The accelerometer model is shown in Figure 9 and the 1st mode shape in Figure 10(a). The modal analysis were carried out with the accelerometer base is fixed. The mode shape shows that the moving fingers act as a beam resulting in the distance between the moving and fixed finger become nonlinear. As can be seen in Figure 10 (b) where the mode shape is zoomed, the gap $\mathbf{d_1}$ is not equal to the gap $\mathbf{d_2}$. This finger motion makes the formed capacitors between moving and fixed fingers non parallel capacitors. The non parallel plates have effect on capacitance, sensitivity,

electrostatic force, electrostatic spring constant, and the overall accelerometer operation [17 and 18].

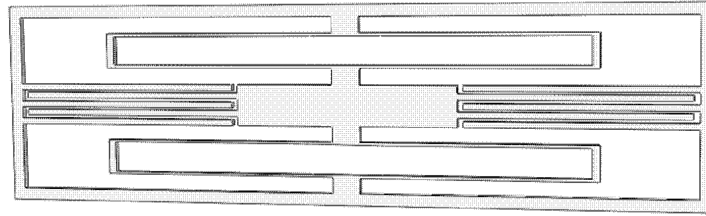

Figure 9 3D model for a typical MEMS accelerometer

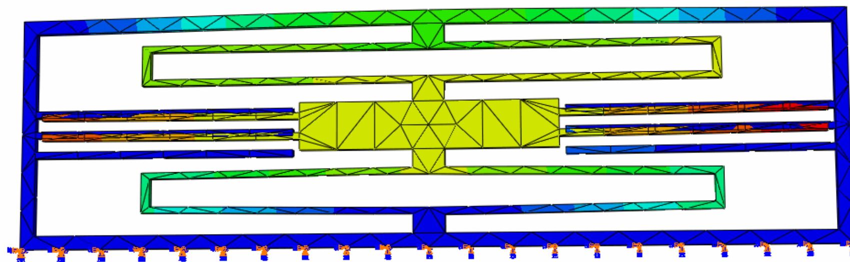

Figure 10 (a). 1st mode shape in vertical direction

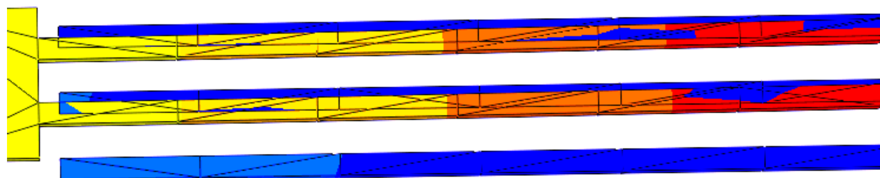

Figure 10 (b) zoomed view

5. In Mechanical Design Possible Improvement :

Having known that the fixed fingers have the rigid body motion, hence a simple model of a MEMS accelerometer has been considered here.

A single spring equivalent to the upper and lower springs shown in Figure 2 has been assumed and just two moving fingers (one on each side of the mass) were used instead of number of fingers. The simplified model is shown in Figure 11. Table 1 lists the physical dimensions and material properties of the model parameters which are partially taken from [22].

Table 1: Physical dimensions and material properties of the MEMS accelerometer

Model Parameters	Dimensions
Mass (m_p)	0.42 ng
Movable finger width (**W_f**)	4 µm
Movable finger length (**L_f**)	160 µm
Movable finger thickness (**t**)	4 µm
Equivalent spring stiffness **k**	1.874 N/m
Young's modulus of poly-Si	$1.70\times10^{11} Pa$
Density of ploy-Si	$2.33\times10^{3} kg/m^{3}$

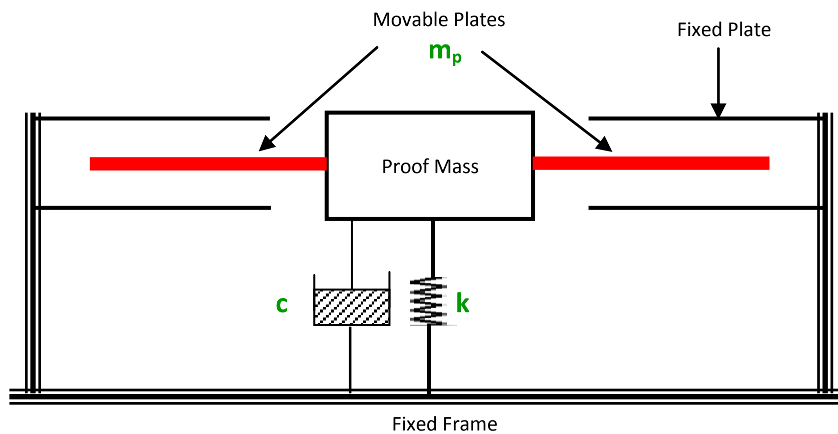

Figure 11 Simple model

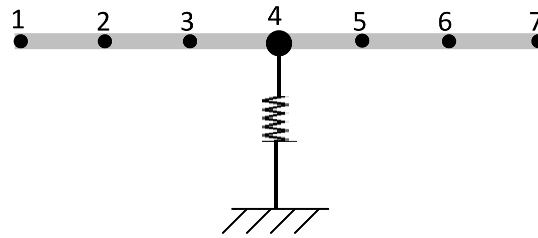

Figure 12 FE Model

The Finite Element (FE) modelling approach has been used to model the mechanical parts of the accelerometer. The finger has been modelled like beam using a 2-node beam element divided into 6 elements; the proof mass and the equivalent spring stiffness have been added at node-4. The FE model is shown in Figure 12. The modal analysis of the FE model has been carried out to find out the natural frequencies and mode shapes. Figure 13 shows the first three mode shapes for this model. The 1st mode natural frequency calculated at 10.631 kHz which can be considered as the natural frequency of the MEMS accelerometer, hence, the working range for this accelerometer should be up to 2 kHz (often 1/5th of the natural frequency).

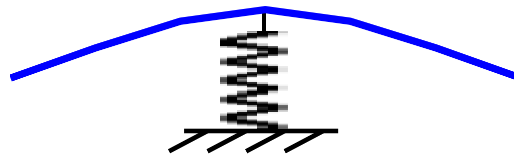

Figure 13 Mode shape at Mode 1: 10.631 kHz

As can be seen, the fingers behave as the cantilever beam at mode 1 which may leads to the effect of non-parallel-plates. Hence, it can be suspected as the reason of observed measurement errors. Therefore, modification to the original finger design has been carried out using

trapezoidal shape of the fingers to achieve rigid body motion. The proposed finger shape is shown in Figure 14. Four different dimensions have been used for the shape thicknesses as listed in Table 2.

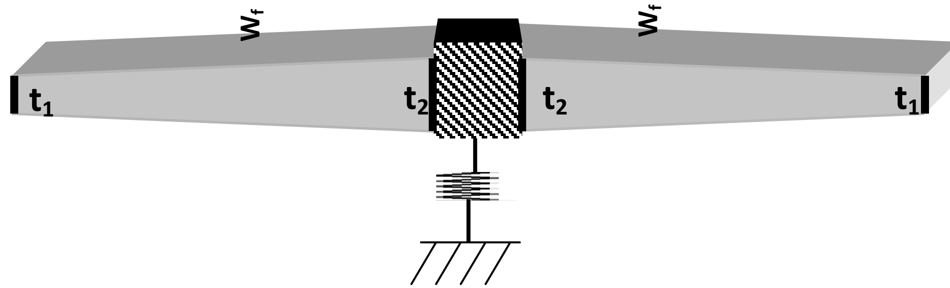

Figure 14 Modified design

Table 2 Dimensions of modified designs and expected improvement

	t_1 (µm)	t_2 (µm)	Expected improvement %
Original	4	4	
Modification 1	3	5	28.17
Modification 2	2	6	54.93
Modification 3	1	7	66.76
Modification 4	0.5	8	67.32

The modal analysis of the FE model for the modified finger design has been carried out. The natural frequencies of each mode for the modified designs are listed in Table 3. As can be seen from Table 4, these modifications in finger design have no affect on the natural frequency of the 1st mode. However, natural frequencies for modes 2 and 3 have been changed due to these modifications (changes in dimensions).

Table 3 Natural frequencies for mode shapes of modified designs

	Natural frequencies, kHz				
Mode	**Original**	**Modification 1**	**Modification 2**	**Modification 3**	**Modification 4**
1	10.631	10.631	10.631	10.631	10.631
2	217.53	279.12	346.75	416.83	455.28
3	947.03	986.94	985.20	908.69	696.69

The 1st mode shapes for the modified finger designs compared with 1st mode shape for the original design are shown in Figure 15. Modification 4 showed approximately a rigid body motion as its mode shape shows much small on deflection compared with the original finger design and other modified finger designs. The expected improvement in the MEMS modified accelerometer when compared with the original MEMS accelerometer design has been quantified as

$$Improvement = \frac{\Delta\phi_O - \Delta\phi_M}{\Delta\phi_O} \times 100\% \qquad (4)$$

where, $\Delta\phi_O$ is the difference of the mode shape between the centre and the finger tip at mode 1 for the original finger design and $\Delta\phi_M$ for the modified finger design. As the proposed modifications are trapezoidal shape, they gave different results from square shape. Also, as the proposed modifications are different in dimensions, it is expected that they will give different results. The calculated '*Improvement*' for the different modifications proposed in Table 2 shows that Modification 4 provides 67% improvement for the present case. An optimised result can be achieved by optimization of different parameters of the accelerometer in Table 1.

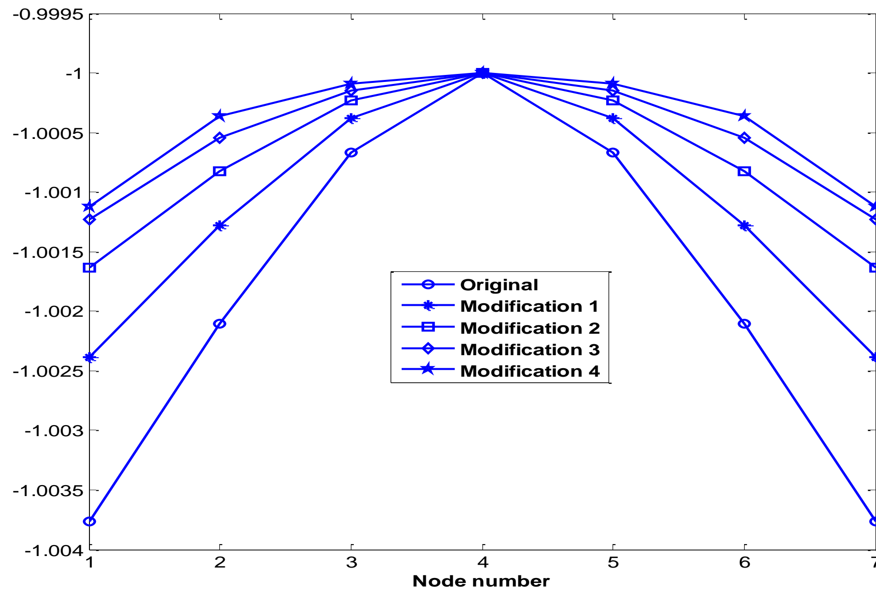

Figure 15 Comparison between the modified finger design and the original one (The original is the one with dimension shown in Table1 which is square shape)

6. Conclusions:

Earlier experimental studies for performance of capacitive type MEMS accelerometers showed deviation in their responses both in amplitude and phase. Modal analysis for a MEMS accelerometer using a simple FE model has been presented. The modal analysis confirms that the accelerometer fingers behave as cantilever beam which can be considered as one of major reasons for the error observed in the vibration measurements. Few modifications on finger shape design have been suggested and showed remarkable improvement. However, it is expected that translating the fingers movement into changes in capacitance and then into output voltage will also introduce some errors.

References :

1. *Barth, P.W.; Pourahmadi, F.; Mayer, R.; Poydock, J.; Petersen, K. A monolithic silicon accelerometer with integral air damping and over range protection, Solid- State Sensor and Actuator Workshop, in Dig. Tech., IEEE 1988, 35 – 38.*
2. *Dong, H.; Jia, Y.; Hao, Y.; Shen, S.; A novel out-of-plane MEMS tunneling accelerometer, Sensors and Actuators A: Physical 2005, volume 120, 360-364.*
3. *Ferrari, V.; Ghisla, A.; Marioli D.; Taroni, A. MEMS ACCELEROMETER WITH MULTIAXIAL RESPONSE BY DYNAMIC RECONFIGURATION OF PIEZORESISTIVE BRIDGES, in Proc., Eurosensors Conference, Sweden, 2006, ISBN/ISSN:97891-631-9281-4.*
4. *Plaza, J.; Collado, A.; Cabruja, E.; Esteve, J. Piezoresistive accelerometers for MCM package, J. Microelectromech. Syst. 2002, volume 11, no. 6, 794–801.*
5. *Xie, H.; Fedder, G. CMOS z-axis capacitive accelerometer with comb-finger sensing, in Proc., IEEE Micro Electro Mechanical Systems (MEMS) 2000, 496–501.*
6. *Coultate, J. K.; Fox, C. H. J.; McWilliam, S.; Malvern, A. R.; Application of optimal and robust design methods to a MEMS accelerometer, Sensors and Actuators A: 2008, 142, 88-96.*
7. *Boga, B.; Ocak, I. E.; Kulah, H.; Akin T. Modelling of a Capacitive Σ-Δ MEMS accelerometer system including the noise components and verification with test results", MEMS 2009, IEEE 22nd Int. Conf. 2009, 821-824.*

8. *Sun, C.; Wang, C.; Fang, W. On the sensitivity improvement of CMOS capacitive accelerometer, Sensors and Actuators A: 2008, 141, 347-352.*
9. *Acar, C. ; Shkel, A. M. Experimental evaluation and comparative analysis of commercial variable-capacitance MEMS accelerometers, J. Micromech. Microeng. 2003, 13, 634-645.*
10. *Lyshevski, S. E. MEMS AND NEMS Systems, Devices and Structures", CRC PRESS LLC, Boca Raton, USA, 2001.*
11. *Thanagasundram, S.; Schlindwein, F. Comparison of integrated micro-electrical-mechanical system and piezoelectric accelerometers for machine condition monitoring, IMechE J. Mechanical Engineering Science Part C 2006, 220, 1135-1146.*
12. *Badri A., Sinha J. K., Albarbar A., Enhancing the frequency range of measurement for an accelerometer, Noise & Vibration Worldwide, Volume 40, Number 6, June 2009 , pp. 33-36.*
13. *Albarbar, A.; Badri, A.; Sinha, J. K.; Starr, A. Performance evaluation of MEMS accelerometers, Measurement 2009, volume 42, no. 5, 790-795.*
14. *ERİŞMİŞ M. A. MEMS Accelerometers and Gyroscopes for Inertial Measurement Units, MSc Thesis, The Graduate School of Natural and Applied Sciences of Middle East Technical University, 2004*
15. *Badri A. E., Sinha J. K. Correcting Amplitude and Phase Measurement of Accelerometer in Frequency Domain, Proceeding of The Fifth International Conference on Condition Monitoring & Machinery Failure Prevention Technologies 2008, 94-100.*
16. *Badri A. E., Sinha J. K. Improvement of Measured Signals of MEMS Accelerometer, 3rd International Conference on Integrity, Reliability*

and Failure, Porto/Portugal, 20-24 July 2009, Paper Ref: S1146_P0507.

17. *F E H Tay, Xu Jun, Y C Liang, V J Logeeswaran and Yao Yufeng, The effects of non-parallel plates in a differential capacitive microaccelerometer, J. Micromech. Microeng. 9 (1999) 283–293.*
18. *Linxi Donga, Lufeng Cheb, Lingling Suna and Yuelin Wang, Effects of non-parallel combs on reliable operation conditions of capacitive inertial sensor for step and shock signals, Sensors and Actuators A 121 (2005) 395–404.*
19. *Asrulnizam Bin Abd Manaf , Yoshinori Matsumoto, Low voltage charge-balanced capacitance–voltage conversion circuit for one-side-electrode-type fluid-based inclination sensor, Solid-State Electronics 53 (2009) 63–69.*
20. *Simon Haykin, "Communication Systems", 4th edition, John Wiley & Sons, Inc, USA, 2001, pp. 90-96.*
21. *Maziar Tavakoli, Rahul Sarpeshkar, An Offset-Canceling Low-Noise Lock-In Architecture for Capacitive Sensing, IEEE Journal of Solid-State Circuits, Vol. 38, No. 2, February 2003.*
22. *Sharma K., Macwan I. G., Zhang L., Hmurcik L., Xiong X. Design Optimization of MEMS Comb Accelerometer, http://www.asee.org/activities/orgnizations/zones/proceedings/*